Time-delay signature suppression in delayed-feedback semiconductor lasers as a paradigm for feedback control in complex physiological networks

Hong, Yanhua; Zhong, Zhuqiang; Shore, K. Alan

Frontiers in Network Physiology

DOI:
10.3389/fnetp.2023.1330375

Published: 11/01/2024

Peer reviewed version

Time-Delay Signature Suppression Using a Photonic Filter in Delayed Feedback Semiconductor Lasers

Yanhua Hong[1*], Zhuqiang Zhong[2], K. Alan Shore[1]

[1]School of Computer Science and Engineering, Bangor University, Bangor LL57 1UT, Wales, UK

[2]College of Science, Chongqing University of Technology, Chongqing 400054, China

*** Correspondence:** y.hong@bangor.ac.uk

Keywords: chaos[1], time delayed feedback[2], feedback control[3], nonlinear dynamics[4], semiconductor lasers[5].

Abstract

Physiological phenomena are often accompanied by time delay effects which may lead to oscillatory and even chaotic dynamics in their behaviors. Analogous dynamics is found in semiconductor lasers subject to delayed optical feedback where the dynamics typically includes a signature of the time delay. In many applications of semiconductor lasers, the suppression of the time delay signature is essential for applications and hence several approaches have been adopted for that purpose. In this paper experimental results are presented wherein photonic filters are utilized in order to suppress time-delay signatures in semiconductor lasers subject to delayed optical feedback effects. Two kinds of semiconductor lasers are used: discrete mode semiconductor lasers and vertical-cavity surface-emitting lasers (VCSELs). It is shown that, by the use of photonic filters, complete suppression of the time-delay signature may be affected in discrete mode semiconductor lasers but that a remnant of the signature persists for VCSELs.

1 Introduction

The study of the effects of time-delay has been identified as an aid to characterizing physiological systems and their regulatory mechanisms. It is found, for example, that oscillations and chaos can be established in blood flow due to time-delay effects (Holstein-Rathlou 1993). Analogous oscillatory and chaotic behavior has been studied in considerable theoretical and experimental detail in semiconductor lasers subject to delayed optical feedback (Soriano et al. 2013). Because of their ease of operation, semiconductor lasers offer a convenient testbed for exploring the diverse dynamical behavior which may arise when the laser is subject to optical feedback (Kane and Shore 2005; Ohtsubo 2013). There is a considerable variety of semiconductor lasers and their response to such time-delayed optical feedback is dependent upon detailed characteristics of the lasers. In turn, such varieties of behavior may be instructive for the exploration of dynamical behaviors arising in physiological systems in which time delay effects play a significant role in the determination of physiological phenomena.

In general, when time delays are the drivers of dynamics, there is a characteristic signature of those delays contained within the system dynamics. The finite time of signal propagation between nodes of a network may manifest itself as a time delay signature (TDS). Such a signature is often undesirable and hence effort has been given to suppression of the TDS. Thus, for example, in the case of chaotic

semiconductor lasers being used for secure communications (Argyris et al. 2005), the persistence of a time delay signature (TDS) may compromise the security of data transmission (Rontani et al. 2009). In this context, substantial efforts have been dedicated to erase time-delay signatures (Shahverdiev and Shore 2009; Nguimdo et al. 2011; Li, Liu, and Chan 2012; Nianqiang Li et al. 2012; Zhong et al. 2013; Hong 2013; A. Wang et al. 2013; Xiang et al. 2014; Hong, Spencer, and Shore 2014; Li and Chan 2015; Mu et al. 2016; Hong et al. 2016; D. Wang et al. 2017; J. Zhang et al. 2017; 2018; Li, Li, and Chan 2018; Jiang et al. 2018; Zhao et al. 2019; Ma et al. 2020; R. Zhang et al. 2020; Cui et al. 2022). These efforts encompass various methods, including modulated optoelectronic feedback, distributed feedback from a fiber Bragg grating, phase-modulated feedback, chaos optical injection, mutual injection, cascaded injection, and the influence of factors like fiber scattering and dispersion. Most of these investigations have centered on vertical-cavity surface-emitting lasers (VCSELs) or distributed feedback (DFB) semiconductor lasers.

Recent research, however, has uncovered unique characteristics of chaos generated in discrete mode (DM) semiconductor lasers, demonstrating the possibility of achieving flat broadband chaos through optical feedback under optimized conditions (Chang et al. 2020). However, the study of the TDS of chaos generated in optically injected DM lasers remains unexplored. DM lasers are a distinct type of Fabry–Pérot (FP) lasers that etch a small number of features along the ridge waveguide, modifying the cavity spectrum to amplify a single cavity mode while suppressing others, ensuring single-mode operation (Osborne et al. 2007). DM lasers offer several advantages, including cost-effectiveness, resilience to optical feedback, stable single mode emission, a broad operational temperature range, and high bandwidth. In this paper, a novel approach to eliminate time delay signatures by using photonic filters in a DM laser is explored. To facilitate comparison, the same experimental configuration is applied to a VCSEL. The findings of this study underscore the exceptional efficacy of photonic filters in suppressing time-delay signatures in DM lasers, whereas in the case of VCSELs, complete signature suppression remains elusive.

2 Experimental setup

The schematic experimental setup is shown in Figure 1. In the experiment, two distinct types of laser diodes (LD) are employed to conduct the experiment. Firstly, we utilize a discrete mode (DM) laser (EP1550-DM-01-FA) from Eblana Photonics. Secondly, we employ VCSELs of the RayCan RC330001-FFA type. Both LDs are driven by a low-noise current source (Thorlabs LDC201 CU) and maintained at room temperature stability through a highly precise temperature controller (Lightwave LDT-5412) and the lasing wavelengths are around 1550 nm.

For the conventional feedback setup, the feedback loop is formed by an optical circulator (OC), fiber couplers (FC1 and FC2), a semiconductor optical amplifier (SOA), a variable optical attenuator (VA), and a polarization controller (PC). Within this feedback loop, the SOA serves to amplify the feedback power, the VA is used to adjust the feedback power, and the PC regulates the polarization of the feedback beam to ensure maximum efficiency on the dynamics of the lasers.

In the photonic filter feedback setup, a variable fiber coupler (VFC: Newport F-CPL-1550_N-FA FC3) is integrated into the feedback loop, as indicated by the dashed frame. The photonic filter feedback configuration is established by connecting ports 2 and 4 of the VFC. This arrangement is commonly referred to an infinite impulse response single-source microwave photonic filters (IIR SSMPFs) or fiber ring resonators, and its specification details have been comprehensively discussed in (Capmany, Ortega, and Pastor 2006)

In the detection section, 10% of the optical power is split using FC1 and directed towards an optical spectrum analyzer (OSA: Agilent 86141B with a resolution of 0.06 nm) for optical spectrum measurements. Simultaneously, FC2 separates 50% of the power from the feedback loop and directs it to a third fiber coupler (FC3). FC3 further divides the optical power evenly and routes it to two photodetectors: a 12 GHz photodetector (PD1: New Focus 1544-B) and a 40 GHz photodetector (PD2: Thorlabs, RXM40AF). The outputs of PD1 and PD2 are recorded by an oscilloscope (OSC, Tektronix TDS 7404) with a bandwidth of 4 GHz and an electrical spectrum analyzer (RF, R&S FSEK20) with a bandwidth of 40 GHz, respectively. The oscilloscope operates at a sampling rate of 20 GS/s, with a total time duration of 2 μs.

In this paper, the optical feedback ratio is defined as the ratio of the feedback power to the output power of the free-running laser. The optical feedback power is the power of the feedback beam before it enters the laser. It is measured at port 1 of the OC, taking into consideration the loss from port 1 to port 2 of the OC. In the experiment, we also investigate the effect of the coupling ratio of the VFC on the TDS. The coupling ratio is defined as the percentage of the power transferred from port 1 to port 4 in the VFC, as shown in Figure 1.

3 Time Delay Signature Analysis Methods

Numerous techniques are available for a qualitative assessment of the TDS, for example, mutual information (Rontani et al. 2009; Nguimdo et al. 2011; N. Li et al. 2012; Li and Chan 2015; D. Wang et al. 2017; J. Zhang et al. 2017), autocorrelation coefficient (ACC)(Rontani et al. 2009; Shahverdiev and Shore 2009; Li, Liu, and Chan 2012; N. Li et al. 2012; Zhong et al. 2013; Hong 2013; A. Wang et al. 2013; Xiang et al. 2014; Hong, Spencer, and Shore 2014; Li and Chan 2015; Mu et al. 2016; Hong et al. 2016; D. Wang et al. 2017; J. Zhang et al. 2017; 2018; Li, Li, and Chan 2018; Jiang et al. 2018; Zhao et al. 2019; Ma et al. 2020; R. Zhang et al. 2020; Cui et al. 2022), permutation entropy (PE)(Zhong et al. 2013; Hong 2013; Xiang et al. 2014; Mu et al. 2016; Cui et al. 2022). In this study, we utilize both the ACC and PE methods to detect the TDS. The ACC, denoted as C is defined as follows

$$C(\Delta t)=\frac{\left\langle\left[I(t+\Delta t)-\left\langle I(t+\Delta t)\right\rangle\right]\left[I(t)-\left\langle I(t)\right\rangle\right]\right\rangle}{\sqrt{\left\langle\left[I(t+\Delta t)-\left\langle I(t+\Delta t)\right\rangle\right]^{2}\right\rangle\left\langle\left[I(t)-\left\langle I(t)\right\rangle\right]^{2}\right\rangle}} \tag{105}$$

where I represents the output intensity of the laser, <·> denotes a time average, and Δt is the delay time. The value of C falls within the range of -1 to 1. A value of 1 signifies complete positive correlation, while -1 indicates full negative (anti) correlation. When the value is 0, it denotes a state of complete randomness, indicating no correlation whatsoever.

The PE method, initially introduced by Bandt and Pompe (Bandt and Pompe 2002), involves a time series $\{I_t, t=1, 2, \ldots, N\}$, which represents the measures N samples of the output intensities of the laser. Given the time series $\{I_t, t=1,2, \ldots, N\}$, subsets S_q, each containing M samples (M>1) of the measured intensities, are formed with an embedding delay time $\tau = nT_s$, where n is an integer number and T_s is the reciprocal of the sampling rate. The ordinal patterns of subsets are expressed as $S_q = [I(t), I(t+\tau), \ldots I(t+(M-1)\tau)]$. For practical purposes, Bandt and Pompe recommended choosing M within the range of 3 to 7. In this work, we have selected M to be 5. Each subset S_q can be organized as $[I(t+(r_1-1)\tau)\leq I(t+(r_2-1)\tau)\leq\ldots\leq I(t+(r_M-1)\tau)]$. Thus, each subset can be uniquely represented as an "ordinal

pattern" $\pi = (r_1, r_2, \ldots, r_M)$, which is one of the possible permutations of subset S_q with M dimensions. The permutation entropy is derived from the probability distribution $p(\pi)$ as follows:

$$p(\pi) = \frac{\#\left\{t \middle| t \le N - M - n + 1; S_q \ has \ type \ \pi\right\}}{N - M - n + 1}$$

where the symbol # denotes "number". The permutation entropy is then determined using the probability $p(\pi)$:

$$h(p) = -\sum p(\pi) \log p(\pi)$$

4 Results

4.1 Discrete Mode (DM) Laser

The DM laser used in this experiment has a threshold current of 12.5 mA at room temperature and is biased at 80 mA. Initially, conventional optical feedback is introduced by disconnecting ports 2 and 4 of the VFC.

Figure 2 shows the time traces (top row), autocorrelation coefficient curves (middle row) and the PE curves (bottom row) of the output of the DM laser subject to optical feedback. The left, middle and right columns are for the feedback ratio of -14.5 dB, -10.5 dB and -1.5 dB, respectively. In Figure 2(A), the red line represents the DM laser's time trace without optical feedback. From the time traces in Figure 2, it can be seen that the laser exhibits random fluctuations in all three feedback ratios, indicating chaos dynamics. To identify the TDS, their corresponding autocorrelation coefficient C as a function of the delay time are calculated and shown in the middle row of Figure 2. At a feedback ratio of -14.6 dB (Figure 2(D)), a significant peak occurs at around 116.8ns, corresponding to the feedback round trip time (τ_1), is observed. This peak, referred to as TDS, is quantified using the peak value of the autocorrelation coefficient at around the feedback round trip time (C_p). For Figure 2(D), the TDS is approximately 0.82. As the feedback ratio increases to -10.5dB, the TDS decreases to about 0.39, as shown in Figure 2(E). Further increasing the feedback ratio to -1.5 dB results in a reduced TDS of approximately 0.2, as depicted in Figure 2(F).

We also utilize PE to investigate the TDS, as shown in the bottom row of Figure 2. In Figure 2(G-I), many troughs attributable to harmonics and sub-harmonics of the feedback round trip time can be observed. Notably, the deepest troughs, occurring around $\tau_1 \approx 116.8$ ns, are less pronounced in the PE analysis compared to the autocorrelation coefficient analysis (middle row of Figure 2). Therefore, we focus on the autocorrelation coefficient for the remaining investigation.

The peak value of the autocorrelation coefficient at the feedback round trip time as a function of the feedback ratio is calculated and presented in Figure 3. The result indicates that the TDS decreases as the feedback ratio increases when the feedback ratio is less than approximately -7 dB. Beyond this threshold, the TDS begins to rise as the feedback ratio increases, peaking around a feedback ratio of -3.5 dB. Subsequently, with further increases in the feedback ratio, the TDS diminishes once more. Notably, the minimum TDS of 0.24 is achieved at the maximum feedback ratio of -1.5 dB. This is corroborated by the autocorrelation coefficient curve displayed in Figure 2(F), which distinctly identifies the time delay signature at 116. 8 ns.

Moving to photonic filter feedback, we connect port ports 2 and 4 of the VFC. Initially, the coupling ratio is set at 50%, equally splitting the powers between ports 3 and 4. In Figure 4, the time traces (upper row) and autocorrelation coefficient curves (bottom row) are presented for the DM laser with photonic filter feedback. The feedback ratios for the left, middle and right columns in Figure 4 match those in Figure 2: -14.5 dB, -10.5 dB, and -1.5 dB, respectively. The red line in Figure 4(A) corresponds to the free-running DM laser's output.

Similar to conventional feedback, the laser exhibits random fluctuations in all three feedback ratios, indicative of chaotic dynamics. The corresponding autocorrelation coefficient curves are displayed in the bottom row of Figure 4. In Figure 4(D), aside from the highest peak at approximately 116.8ns, smaller peaks appear around 20.5 ns, 127.05 ns and 137.3ns. These additional peaks are attributed to the time delay introduced by the ring cavity recirculation. Each recirculation within the ring cavity introduces a delay time (τ_2) of approximately 10.25ns. The highest peak has a value of approximately 0.68. In the case of -10.5 dB feedback ratio, as shown in Figure 4(E), the maximum peak value decreases to about 0.37. When the feedback ratio increases to approximately -1.5dB, as demonstrated in Figure 4(F), no distinguishable peaks are observed. The TDS has been completely concealed.

The maximum peak value of the autocorrelation coefficient at the feedback round trip times (τ_1, $\tau_1+\tau_2$, $\tau_1+2\tau_2$, $2\tau_2$, or other combinations) as a function of the feedback ratio is presented in Figure 5. The result demonstrates a consistent decrease in the TDS as the feedback ratio increases. When the feedback ratio reaches approximately -2.0dB, the TDS value is approximately 0.03. Further increases in the feedback ratio yield minimal changes in TDS due to the absence of distinguishable peaks in the autocorrelation curves.

The influence of the coupling ratio of the photonic filter on the time delay signature is also explored. In Figure 6, curve A represents the scenario with conventional feedback, while the remaining curves correspond to setups involving photonic optical feedback, each with different coupling ratios. It is evident that at lower feedback ratios, photonic filter feedback does not show any advantage in suppressing the TDS compared to conventional feedback. However, as the optical feedback intensity increases, the addition of photonic filter feedback proves advantageous in suppressing the TDS, particularly when the coupling ratio approaches 50%.

4.2 VCSELs

To investigate whether the concealment of the TDS is solely attributable to photonic filter feedback, we conducted a similar experiment using a VCSEL. The threshold current of the VCSEL used in the experiment is 1.8 mA at the room temperature and is biased at 4 mA. Figure 7 displays the TDS as a function of the feedback ratio in the VCSEL with various coupling ratios. Notably, the addition of photonic filter feedback at coupling ratios of 50% or 72% effectively suppressed TDS across all feedback ratios, which is similar to the results observed in DFB lasers (Cui et al. 2022). However, for coupling ratios below 13%, the TDS exhibit little deviation from conventional optical feedback, in contrast to DM lasers, where TDS suppression with photonic filter feedback is primarily observed at higher feedback ratios. Remarkably, even a lower coupling ratio as 7% still significantly contributes to TDS suppression in DM lasers at higher feedback ratios. The optimal coupling ratio for TDS suppression in the VCSEL is determined to be 72%. The minimum TDS achieved in the VCSEL is

approximately 0.12 at a feedback ratio of around 1.0 dB with the coupling ratio of 72%, which is higher than the minimum TDS of 0.03 observed in the DM laser.

Figure 8 presents the autocorrelation coefficient curve obtained under the influence of photonic filter feedback with optimal coupling ratio and the optical feedback ratio in the VCSEL. This curve exhibits three distinct peaks, with delay times of approximately 10.25ns, 112.45ns and 122.7ns, corresponding to τ_2, τ_1, and $\tau_1+\tau_2$, respectively. This observation indicates that the presence of photonic filter feedback in the VCSEL is unable to entirely eliminate TDS.

5 Conclusion

In this study, we conducted experimental investigations into the TDS of semiconductor lasers under conventional feedback and photonic filter feedback conditions. Specifically, two types of semiconductor lasers, namely, DM lasers and VCSELs, are comprehensively examined. Our findings highlight the substantial advantages of photonic filter feedback in TDS suppression, particularly evident in the case of DM lasers. At the optimal coupling ratio and optical feedback ratio, we achieved remarkable TDS reduction, with the TDS minimized to as low as 0.03, effectively concealed within the background noise. For DM lasers, the benefits of photonic filter feedback in TDS suppression manifest primarily at higher feedback ratios. Conversely, in the case of VCSELs, photonic filter feedback proves advantageous across a wider spectrum of feedback ratios, particularly in the coupling ratio range of approximately 50% to 72%. Nevertheless, it is worth noting that in VCSELs, while photonic filter feedback induces significant TDS suppression with an appropriate coupling ratio, a residual TDS signature remains discernible. The reason the photonic filter can suppress the TDS is that the photonic filter feedback is equivalent to optical feedback from multiple external cavities with different lengths, and due to the multiple Vernier effect, the TDS is suppressed. The disparity between DM lasers and VCSELs can be attributed to their respective laser structures. DM lasers feature multiple etching features along the ridge waveguide, which alter the characteristics of the laser spectrum. This modification, in turn, mitigates the occurrence of recurring features induced by optical feedback. Combining the multiple Vernier effect with the modified laser spectrum totally conceals the TDS in the discrete mode laser with photonic filter feedback. However, the effectiveness of photonic filter feedback for TDS suppression is diminished in VCSELs because they lack the same special spectrum characteristics as discrete mode lasers. Without the specific spectrum provided by the multiple etching features along the ridge waveguide, the photonic filter cannot totally suppress the TDS in VCSELs.

This research serves not only to enhance our comprehension of TDS control in semiconductor lasers but also holds significance in the context of physiological phenomena. Physiological processes often exhibit time delay effects, which can contribute to oscillatory and even chaotic dynamics in their behaviors. The insights gained from this study can contribute to the better understanding and management of physiological phenomena marked by time-delayed feedback, opening new avenues for research and applications in the realm of controlling and regulating complex physiological systems.

Data Availability Statement

Datasets are available on request:

The raw data supporting the conclusions of this article will be made available by the authors, without undue reservation.

Conflict of Interest

The authors declare that the research was conducted in the absence of any commercial or financial relationships that could be construed as a potential conflict of interest.

6 Author Contributions

YH: Conceptualization, Data curation, Formal Analysis, Investigation, Methodology, Software, Writing–original draft, Writing–review and editing. ZQZ: Data curation, Formal Analysis, Project administration, Writing–review and editing. KAS: Data curation, Writing–original draft, Writing–review and editing.

7 Funding

This work was supported in part by the National Natural Science Foundation of China under Grants 62205040, 62265016, in part by the Research and Innovation Team Cultivation Program of Chongqing University of Technology under Grants 2023TDZ007.

References

Argyris, Apostolos, Dimitris Syvridis, Laurent Larger, Valerio Annovazzi-Lodi, Pere Colet, Ingo Fischer, Jordi García-Ojalvo, Claudio R. Mirasso, Luis Pesquera, and K. Alan Shore. 2005. 'Chaos-Based Communications at High Bit Rates Using Commercial Fibre-Optic Links'. *Nature* 438 (7066): 343–46. https://doi.org/10.1038/nature04275.

Bandt, Christoph, and Bernd Pompe. 2002. 'Permutation Entropy: A Natural Complexity Measure for Time Series'. *Physical Review Letters* 88 (17): 174102. https://doi.org/10.1103/PhysRevLett.88.174102.

Capmany, J., B. Ortega, and D. Pastor. 2006. 'A Tutorial on Microwave Photonic Filters'. *Journal of Lightwave Technology* 24 (1): 201–29. https://doi.org/10.1109/JLT.2005.860478.

Chang, Da, Zhuqiang Zhong, Jianming Tang, Paul S. Spencer, and Yanhua Hong. 2020. 'Flat Broadband Chaos Generation in a Discrete-Mode Laser Subject to Optical Feedback'. *Optics Express* 28 (26): 39076. https://doi.org/10.1364/OE.413674.

Cui, Bing, Guangqiong Xia, Xi Tang, Fei Wang, Zaifu Jiang, Yanfei Zheng, Fengling Zhang, and Zhengmao Wu. 2022. 'Generation of Chaotic Signals With Concealed Time-Delay Signature Based on a Semiconductor Laser Under Multi-Path Optical Feedback'. *IEEE Photonics Journal* 14 (1): 1504605. https://doi.org/10.1109/JPHOT.2021.3133659.

Holstein-Rathlou, N H. 1993. 'Oscillations and Chaos in Renal Blood Flow Control.' *Journal of the American Society of Nephrology* 4 (6): 1275–87. https://doi.org/10.1681/ASN.V461275.

Hong, Yanhua. 2013. 'Experimental Study of Time-Delay Signature of Chaos in Mutually Coupled Vertical-Cavity Surface-Emitting Lasers Subject to Polarization Optical Injection'. *Optics Express* 21 (15): 17894. https://doi.org/10.1364/OE.21.017894.

Hong, Yanhua, Ana Quirce, Bingjie Wang, Songkun Ji, Krassimir Panajotov, and Paul S. Spencer. 2016. 'Concealment of Chaos Time-Delay Signature in Three-Cascaded Vertical-Cavity Surface-Emitting Lasers'. *IEEE Journal of Quantum Electronics* 52 (8): 2400508. https://doi.org/10.1109/JQE.2016.2587099.

Hong, Yanhua, Paul S. Spencer, and K. Alan Shore. 2014. 'Wideband Chaos With Time-Delay Concealment in Vertical-Cavity Surface-Emitting Lasers With Optical Feedback and Injection'. *IEEE Journal of Quantum Electronics* 50 (4): 236–42. https://doi.org/10.1109/JQE.2014.2304745.

Jiang, Ning, Anke Zhao, Shiqin Liu, Chenpeng Xue, Boyang Wang, and Kun Qiu. 2018. 'Generation of Broadband Chaos with Perfect Time Delay Signature Suppression by Using Self-Phase-Modulated Feedback and a Microsphere Resonator'. *Optics Letters* 43 (21): 5359. https://doi.org/10.1364/OL.43.005359.

Kane, Deborah M., and K. Alan Shore, eds. 2005. *Unlocking Dynamical Diversity: Optical Feedback Effects on Semiconductor Lasers*. Chichester ; Hoboken, NJ: Wiley.

Li, Nianqiang, Wei Pan, Shuiying Xiang, Lianshan Yan, Bin Luo, and Xihua Zou. 2012. 'Loss of Time Delay Signature in Broadband Cascade-Coupled Semiconductor Lasers'. *IEEE Photonics Technology Letters* 24 (23): 2187–90. https://doi.org/10.1109/LPT.2012.2225101.

Li, Song-Sui, Qing Liu, and Sze-Chun Chan. 2012. 'Distributed Feedbacks for Time-Delay Signature Suppression of Chaos Generated From a Semiconductor Laser'. *IEEE Photonics Journal* 4 (5): 1930–35. https://doi.org/10.1109/JPHOT.2012.2220759.

Li, Song-Sui, and Sze-Chun Chan. 2015. 'Chaotic Time-Delay Signature Suppression in a Semiconductor Laser With Frequency-Detuned Grating Feedback'. *IEEE Journal of Selected Topics in Quantum Electronics* 21 (6): 1800812. https://doi.org/10.1109/JSTQE.2015.2427521.

Li, Song-Sui, Xiao-Zhou Li, and Sze-Chun Chan. 2018. 'Chaotic Time-Delay Signature Suppression with Bandwidth Broadening by Fiber Propagation'. *Optics Letters* 43 (19): 4751. https://doi.org/10.1364/OL.43.004751.

Ma, Yuanting, Shuiying Xiang, Xingxing Guo, Ziwei Song, Aijun Wen, and Yue Hao. 2020. 'Time-Delay Signature Concealment of Chaos and Ultrafast Decision Making in Mutually Coupled Semiconductor Lasers with a Phase-Modulated Sagnac Loop'. *Optics Express* 28 (2): 1665. https://doi.org/10.1364/OE.384378.

Mu, Penghua, Wei Pan, Lianshan Yan, Bin Luo, Nianqiang Li, and Mingfeng Xu. 2016. 'Experimental Evidence of Time-Delay Concealment in a DFB Laser With Dual-Chaotic Optical Injections'. *IEEE Photonics Technology Letters* 28 (2): 131–34. https://doi.org/10.1109/LPT.2015.2487519.

Nguimdo, Romain Modeste, Pere Colet, Laurent Larger, and Luís Pesquera. 2011. 'Digital Key for Chaos Communication Performing Time Delay Concealment'. *Physical Review Letters* 107 (3): 034103. https://doi.org/10.1103/PhysRevLett.107.034103.

Ohtsubo, Junji. 2013. *Semiconductor Lasers: Stability, Instability and Chaos*. Vol. 111. Springer Series in Optical Sciences. Berlin, Heidelberg: Springer Berlin Heidelberg. https://doi.org/10.1007/978-3-642-30147-6.

Osborne, S., S. O'Brien, K. Buckley, R. Fehse, A. Amann, J. Patchell, B. Kelly, D.R. Jones, J. O'Gorman, and E.P. O'Reilly. 2007. 'Design of Single-Mode and Two-Color Fabry--PÉrot Lasers With Patterned Refractive Index'. *IEEE Journal of Selected Topics in Quantum Electronics* 13 (5): 1157–63. https://doi.org/10.1109/JSTQE.2007.903851.

Rontani, Damien, Alexandre Locquet, Marc Sciamanna, David S. Citrin, and Silvia Ortin. 2009. 'Time-Delay Identification in a Chaotic Semiconductor Laser With Optical Feedback: A Dynamical Point of View'. *IEEE Journal of Quantum Electronics* 45 (7): 879–1891. https://doi.org/10.1109/JQE.2009.2013116.

Shahverdiev, E.M., and K.A. Shore. 2009. 'Erasure of Time-Delay Signatures in the Output of an Opto-Electronic Feedback Laser with Modulated Delays and Chaos Synchronisation'. *IET Optoelectronics* 3 (6): 326–30. https://doi.org/10.1049/iet-opt.2009.0028.

Soriano, Miguel C., Jordi García-Ojalvo, Claudio R. Mirasso, and Ingo Fischer. 2013. 'Complex Photonics: Dynamics and Applications of Delay-Coupled Semiconductors Lasers'. *Reviews of Modern Physics* 85 (1): 421–70. https://doi.org/10.1103/RevModPhys.85.421.

Wang, Anbang, Yibiao Yang, Bingjie Wang, Beibei Zhang, Lei Li, and Yuncai Wang. 2013. 'Generation of Wideband Chaos with Suppressed Time-Delay Signature by Delayed Self-Interference'. *Optics Express* 21 (7): 8701. https://doi.org/10.1364/OE.21.008701.

Wang, Daming, Longsheng Wang, Tong Zhao, Hua Gao, Yuncai Wang, Xianfeng Chen, and Anbang Wang. 2017. 'Time Delay Signature Elimination of Chaos in a Semiconductor Laser by Dispersive Feedback from a Chirped FBG'. *Optics Express* 25 (10): 10911. https://doi.org/10.1364/OE.25.010911.

Xiang, Shuiying, Wei Pan, Liyue Zhang, Aijun Wen, Lei Shang, Huixing Zhang, and Lin Lin. 2014. 'Phase-Modulated Dual-Path Feedback for Time Delay Signature Suppression from Intensity and Phase Chaos in Semiconductor Laser'. *Optics Communications* 324 (August): 38–46. https://doi.org/10.1016/j.optcom.2014.03.017.

Zhang, Jianzhong, Changkun Feng, Mingjiang Zhang, Yi Liu, and Yongning Zhang. 2017. 'Suppression of Time Delay Signature Based on Brillouin Backscattering of Chaotic Laser'. *IEEE Photonics Journal* 9 (2): 1502408. https://doi.org/10.1109/JPHOT.2017.2690680.

Zhang, Jianzhong, Mengwen Li, Anbang Wang, Mingjiang Zhang, Yongning Ji, and Yuncai Wang. 2018. 'Time-Delay-Signature-Suppressed Broadband Chaos Generated by Scattering Feedback and Optical Injection'. *Applied Optics* 57 (22): 6314. https://doi.org/10.1364/AO.57.006314.

Zhang, Renheng, Pei Zhou, Yigong Yang, Qi Fang, Penghua Mu, and Nianqiang Li. 2020. 'Enhancing Time-Delay Suppression in a Semiconductor Laser with Chaotic Optical Injection via Parameter Mismatch'. *Optics Express* 28 (5): 7197. https://doi.org/10.1364/OE.389831.

Zhao, Anke, Ning Jiang, Shiqin Liu, Chenpeng Xue, and Kun Qiu. 2019. 'Wideband Time Delay Signature-Suppressed Chaos Generation Using Self-Phase-Modulated Feedback Semiconductor Laser Cascaded With Dispersive Component'. *Journal of Lightwave Technology* 37 (19): 5132–39.

Zhong, Zhu-Qiang, Zheng-Mao Wu, Jia-Gui Wu, and Guang-Qiong Xia. 2013. 'Time-Delay Signature Suppression of Polarization-Resolved Chaos Outputs from Two Mutually Coupled VCSELs'. *IEEE Photonics Journal* 5 (2): 1500409–1500409. https://doi.org/10.1109/JPHOT.2013.2252160.

Figure Captions

Figure 1. Experimental setup

Figure 2. The time traces (top row), autocorrelation coefficient curves (middle row) and the PE curves (bottom row) of the output of the DM laser subject to optical feedback. The feedback ratios are -14.5 dB (left column), -10.5 dB (middle column) and -1.5 dB (right column). The red line in Figure 2(**A**) is the free-running DM laser output.

Figure 3. The TDS as a function of the feedback ratio for the conventional feedback.

Figure 4. The time traces (top row) and autocorrelation coefficient curves (bottom row) of the output of the DM laser with photonic filter feedback with the coupling ratio of 50%. The feedback ratios are -14.5 dB (left column), -10.5 dB (middle column) and -1.5 dB (right column). The red line in Figure 4(**A**) is the free-running DM laser output.

Figure 5. TDS as a function of the feedback ratio for the photonic filter feedback with the coupling ratio of 50%.

Figure 6. TDS as a function of the feedback ratio in the DM laser with optical feedback. Curve A is for conventional optical feedback. Curves B, C, D, E, F and G are for photonic filter feedback with the coupling ratio of 7%, 13%, 26%, 50%, 72% and 94%, respectively.

Figure 7. TDS as a function of the feedback ratio in the VCSEL with various coupling ratios.

Figure 8. The autocorrelation coefficient curve of the output of the VCSEL with photonic filter feedback with the coupling ratio of 72% and the feedback ratio of 1.0 dB.

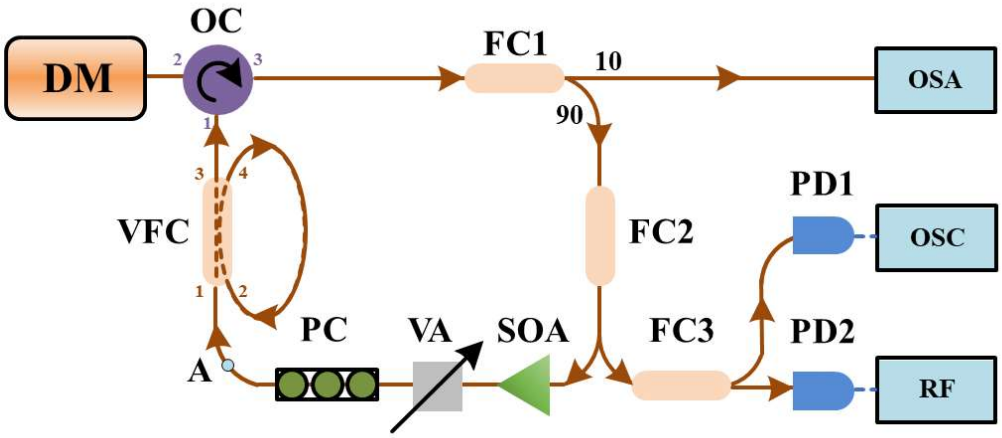

Figure 1. Experimental setup

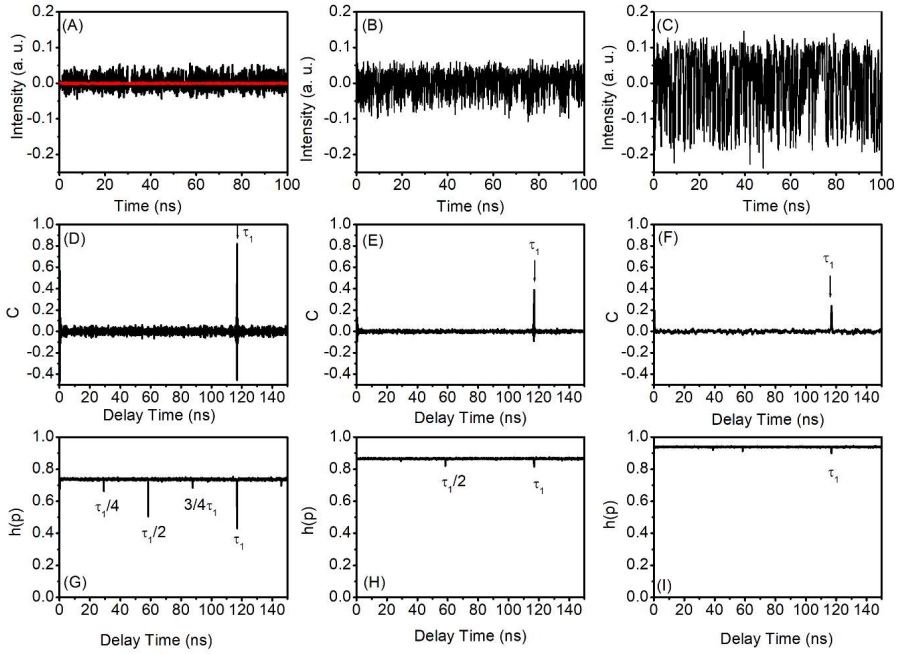

Fig. 2

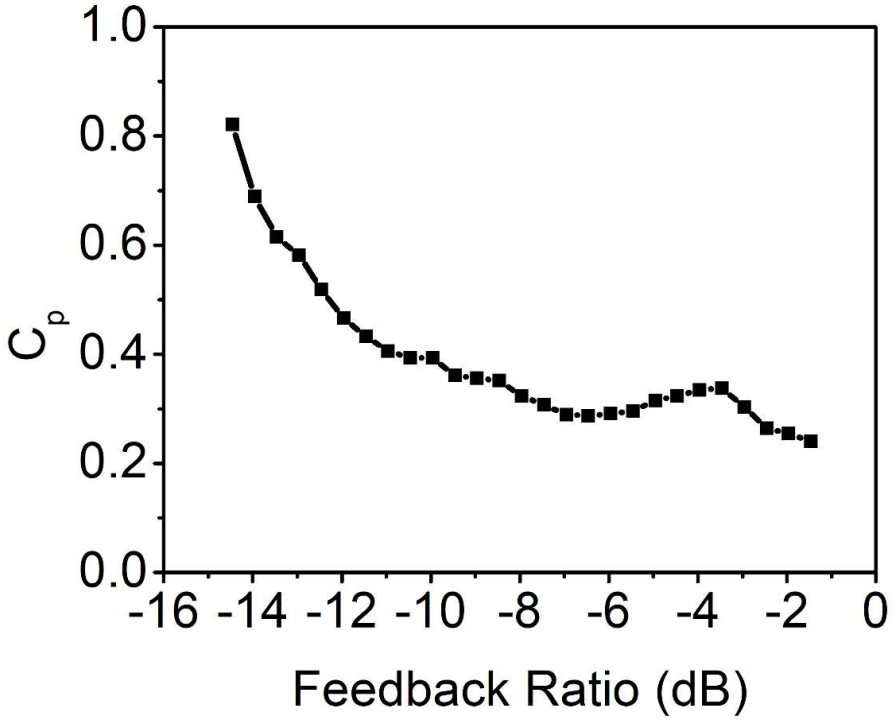

Fig. 3

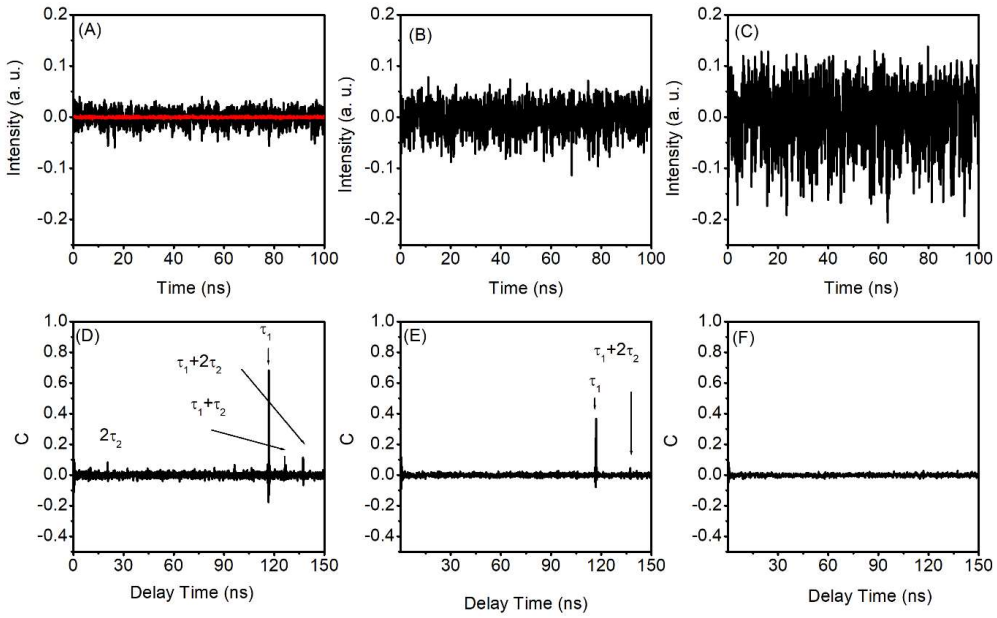

373
374
375

Fig. 4

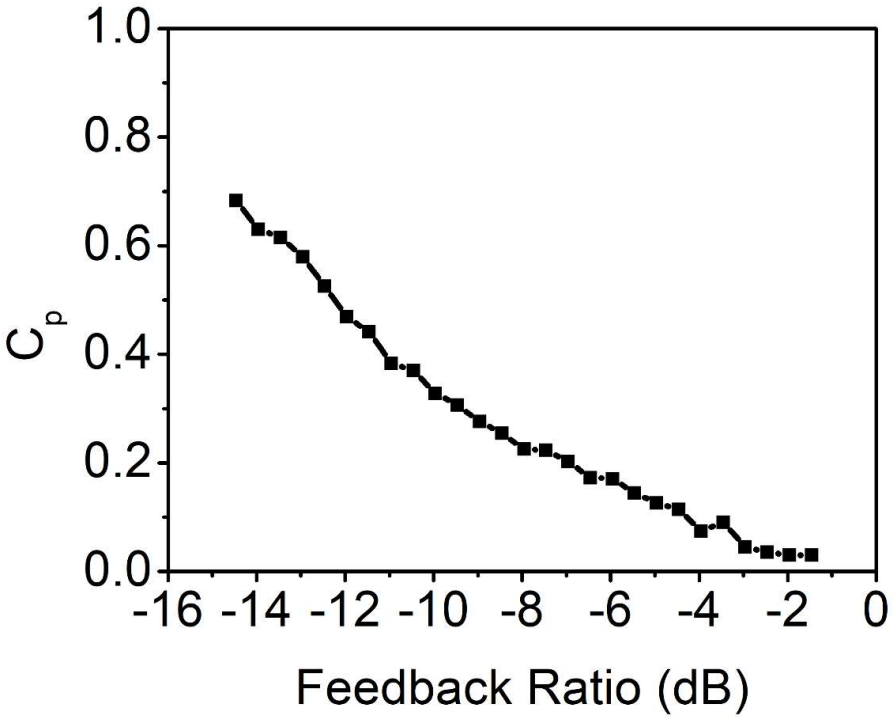

376
377
378

Fig. 5

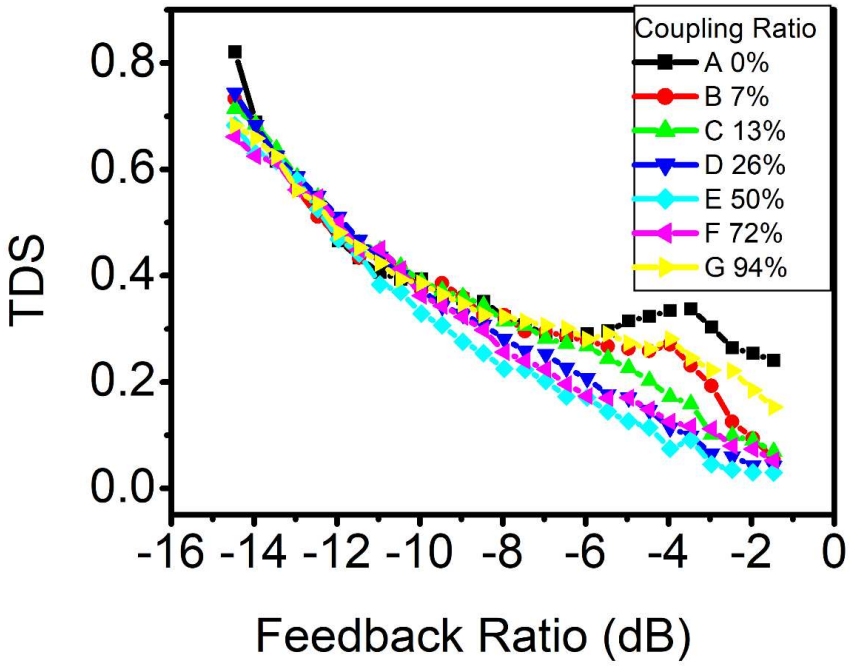

379
380
381

Fig. 6

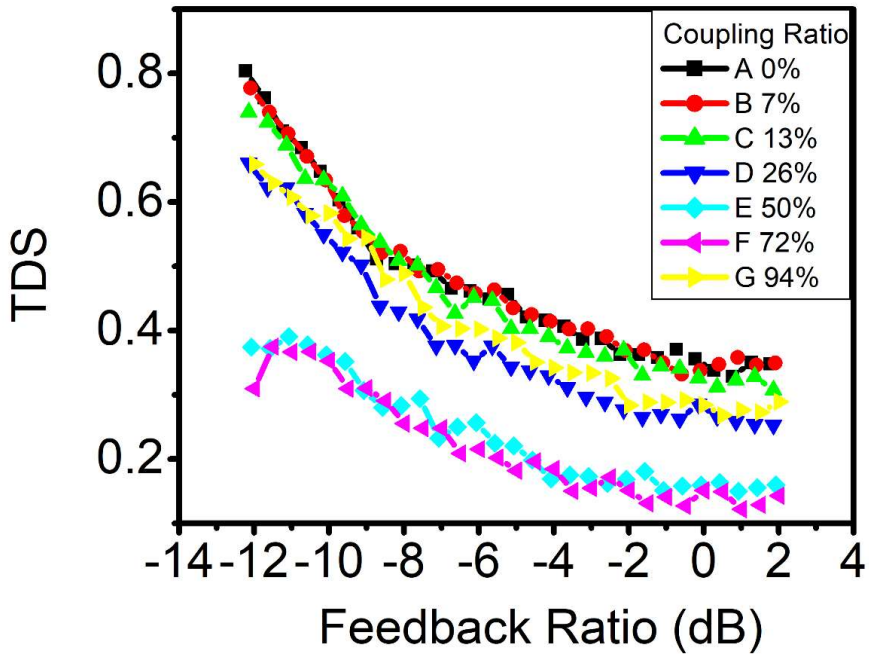

382
383
384

Fig. 7

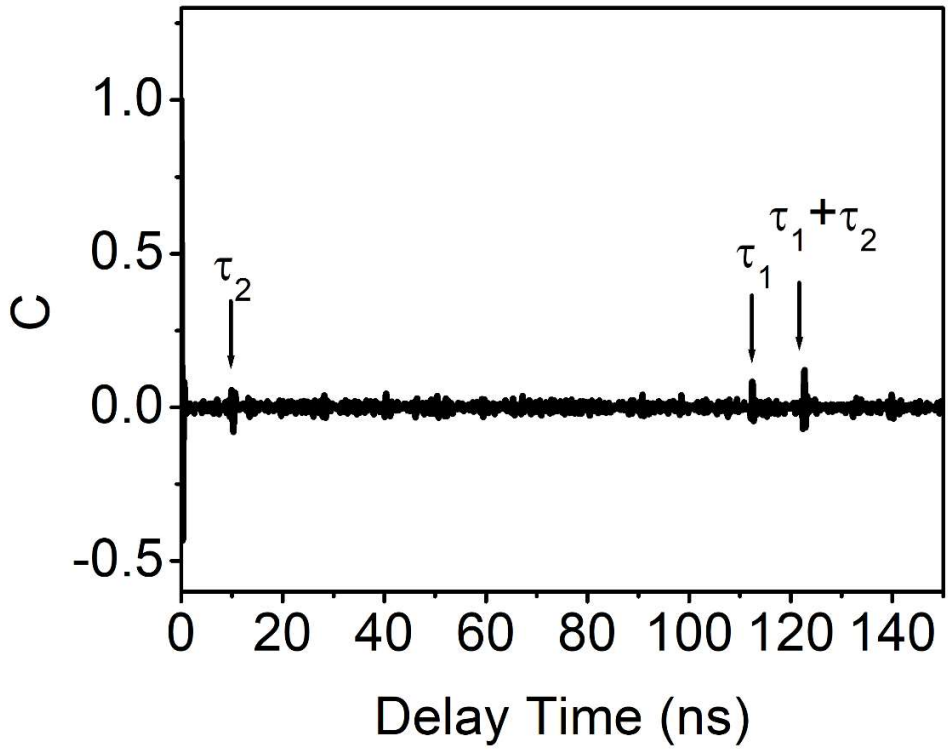

385
386

Fig. 8